Interval Observer Design for Sequestered Erythrocytes Concentration Estimation in Severe Malaria Patients

Kwassi Degue, Denis Efimov, Abderrahman Iggidr

HAL Id: hal-02927467
https://hal.inria.fr/hal-02927467

Interval Observer Design for Sequestered Erythrocytes Concentration Estimation in Severe Malaria Patients

Kwassi H. Degue[a,*], Denis Efimov[b], Abderrahman Iggidr[c]

[a]*Department of Electrical Engineering, Polytechnique Montreal and GERAD, Montreal, QC H3T-1J4, Canada.*
[b]*Inria, Univ. Lille, CNRS, UMR 9189 - CRIStAL, F-59000 Lille, France and Department of Control Systems and Informatics, University ITMO, 197101 Saint Petersburg, Russia.*
[c]*Université de Lorraine, CNRS, Inria, IECL, F-57000 Metz, France.*

Abstract

A child dies from malaria every two minutes worldwide, according to the World Health Organization. When prescribing antimalarial drugs, a challenging problem for physicians consists in estimating sequestered parasites *Plasmodium falciparum* populations from noisy measurements of circulating parasite concentrations, while handling uncertainty. In this article, we design an interval state estimator for uncertain models of malaria patients. We consider the ubiquitous case in which only intervals of admissible values are available for all parameters in the model except for infection rates, whose bounding values are unavailable. Furthermore we compute optimal gains for the interval observer by using linear programming to minimize the estimated interval width. We test the observer's efficiency in simulation for a model and for real measured data collected by the US Public Health Service at the National Institutes of Health laboratories in Columbia, South Carolina and Milledgeville, Georgia.

Keywords: Interval observers, unknown input observers, nonlinear systems, biological system modeling, diseases.

1. Introduction

Malaria is an important life-threatening disease that caused 228 million cases of severe illness and resulted in 405 000 deaths worldwide in 2018, according to

---

*Corresponding author
Email address:* `kwassi-holali.degue@polymtl.ca` (Kwassi H. Degue)

the World Health Organization [1]. The disease is caused by *Plasmodium* parasites, which are spread among the population through bites of infected female *Anopheles mosquitoes*. The most virulent species called *Plasmodium falciparum* are responsible for most malaria-related deaths. Sequestration is characteristic of *Plasmodium falciparum* infections, which is related to the *Plasmodium* life cycle. The cycle begins when a parasite enters the human body. Next, it migrates to the liver and starts to multiply within it. Free forms resulting from this multiplication, the so-called *merozoites*, invade the red blood cells (erythrocytes). The infected erythrocytes grow up during the erythrocytic cycle. At roughly the middle stage of trophozoite development (in 24 hours), molecules on the surface of infected erythrocytes are able to connect to receptors of endothelial cells. An effect of this bind consists of hiding infected erythrocytes within vessels of organs (such as the brain), where they remain until the erythrocytes break and the merozoites are released. During this phase of attachment, called *sequestration*, the infected erythrocytes cannot be detected in the blood flow, they are "sequestered". Moreover, it is difficult to evaluate a reliable response to antimalarial therapies without knowing a priori the sequestered parasite concentration [2, 3]. Since antimalarial drugs act differently depending on the stage of parasite development, it becomes necessary to estimate sequestered parasites concentrations.

Related work. In practice, to determine the stage of infection for a patient, the total parasite concentration $\sum_{i=1}^{n} y_i$ in the bloodstream is required, with y_i representing the population of parasites of certain age, from the youngest y_1 to the oldest y_n and $n > 1$ establishing the grid of age differentiation. However, only the presence of peripheral infected erythrocytes, *i.e.* the young parasites $y_1 + y_2 + ...y_k$ for some $k < n$, also called *circulating*, are detectable on peripheral blood smears. The other ones (sequestered $y_{k+1}, ...y_n$), which are hidden in some organs like brain and heart, cannot be measured. Nowadays, the concentration of sequestered infected cells cannot be measured directly by clinical methods, and the measurements of circulating parasites are rather costly and corrupted by noise. This reasoning explains why the estimation of sequestered parasite population is an important challenge, with many authors having investigated this issue [4, 5]. The estimation methods that are proposed in the existing literature assume that the exact value of the infection rate parameter β is known. This constitutes a real drawback since β is a highly uncertain parameter and this strong assumption decreases efficiency of the proposed estimators in practice. In contrast, control theory can be used to circumvent this

2

issue by designing observers. From the control-theoretic perspective, only [5] has designed a pointwise observer to solve this issue. However, [5] assumed that the measurements of circulating parasites are not corrupted by noise and it assumed that exact values are known for uncertainty on the model parameters of patients, which is a real drawback in practice. In addition, [5] has designed an observer that has difficulties to handle positivity of the estimated values (the estimated variables have to take only positive values since all elements of the state vector for infected patient are concentrations).

Contributions. The novelty of this paper lies in designing an interval observer to estimate interval of admissible values for sequestered parasites populations, for given uncertainty in patient models[1]. In contrast to [5], we consider, for the first time, patient models in which only intervals of admissible values are available for all parameters except for infection rates, whose bounding values are unavailable. Indeed, in practice, uncertainty plays an important impact and needs to be taken into account. In such a case, a conventional estimator converging to the ideal value of the state cannot be synthesized [7, 8]. Therefore, we design an interval estimator that, using input-output information, evaluates the set of admissible values (interval) for the state at each instant of time. The interval length is proportional to the size of the model uncertainty and has to be minimized by tuning the observer parameters. Several approaches to design interval/set-membership estimators have been proposed [9, 10, 11, 12, 13, 14]. This work is devoted to a subclass of set-membership estimators, the so-called interval observers, whose design is based on the monotone systems theory [15, 12, 16, 17, 18, 19, 20, 21, 22]. In contrast to [5], since the estimated variables take positive values, the obtained estimates provided by our observer take positive values only, which poses an additional constraint to satisfy in this rather complex estimation problem. Instead of selecting the observer gains manually as in [5], we optimize these gains by computing linear programs that can be solved by using standard numerical solvers. In addition, instead of assuming that the value of the parameter β is known as in the existing literature, we design an interval observer that does not use such an assumption and we provide a method to estimate lower and upper bounds of this parameter since β is a highly uncertain parameter that cannot be obtained from biological considerations in practice [5, 23]. Moreover, only linear systems and unknown

---

[1]A preliminary version of this research was presented at ECC 2016 [6].

inputs that have no impact on the output are considered in [24]. In contrast, we consider a nonlinear system with unknown inputs that affect the output in this work, leading us to design upper and lower bounds for the uncertain input before constructing an interval observer for the system.

Paper organization. The outline of this paper is as follows. We present the problem statement in Section 2. Section 2 provides some background from the theories of interval estimation, introduces tools to compute norms for signals and systems for the case in which the dynamical model is nonnegative. Section 3 provides some background from the theories of interval estimation, the stability of positive systems and presents some results on non-homogenous sliding mode differentiation. Then, these results are used to design the interval observer after determining upper and lower bounds for the system uncertainties, and to evaluate lower and upper bounds of the uncertain infection rate parameter β. Section 4 describes an efficient methodology to compute the corresponding observer gains while evaluating the closeness of the estimated bounds to the state. Numerical simulations with selected model and really measured data collected by the US Public Health Service at the National Institutes of Health laboratories in Columbia, South Carolina and Milledgeville, Georgia are described in Section 5.

Notation: Throughout the paper, we denote the real numbers by $\mathbb{R}$, $\mathbb{R}_+ = \{\tau \in \mathbb{R} : \tau \geq 0\}$. We denote the cones of positive and nonnegative vectors of dimension n by $\mathbb{R}^n_{>0}$ and $\mathbb{R}^n_+$ respectively. We denote Euclidean norm for a vector $x \in \mathbb{R}^n$ as $|x|$, for $A \in \mathbb{R}^{n \times n}$ the corresponding induced matrix norm as $\|A\|$, and for a measurable and locally essentially bounded input $u : \mathbb{R}_+ \to \mathbb{R}$ the symbol $||u||_{[t_0,t_1]}$ denotes its L_∞ norm

$$||u||_{[t_0,t_1]} = ess \sup_{t \in [t_0,t_1]} |u(t)|,$$

if $t_0 = 0$ and $t_1 = +\infty$ we simply write $||u||_\infty$. We denote as $\mathcal{L}_\infty$ the set of all inputs u with the property $||u||_\infty < \infty$. The symbols I_n, $\mathbb{1}_{n \times m}$ and $\mathbb{1}_p$ denote the identity matrix with dimension $n \times n$, the matrix with all elements equal 1 with dimensions $n \times m$ and $p \times 1$, respectively. For two vectors $x_1, x_2 \in \mathbb{R}^n$ or matrices $A_1, A_2 \in \mathbb{R}^{n \times n}$, the relations $x_1 \leq x_2$ and $A_1 \leq A_2$ are understood elementwise. The relation $P \prec 0$ ($P \succ 0$) means that the matrix $P \in \mathbb{R}^{n \times n}$ is negative (positive) definite. A matrix $A \in \mathbb{R}^{n \times n}$ is Hurwitz if all its eigenvalues have negative real parts; it is called Metzler if all its elements outside of the main

diagonal are nonnegative, *i.e.* if there is $s > 0$ such that $sI_n + A \geq 0$. Given a matrix $A \in \mathbb{R}^{m \times n}$, define $A^+ = \max\{0, A\}$ applied elementwise, $A^- = A^+ - A$ (the same for vectors) and denote the matrix of absolute values of all elements by $|A| = A^+ + A^-$. We denote the set of diagonal matrices of dimension n by $\mathbb{D}^n$ and the subsets of those with positive diagonal entries and nonnegative entries, respectively, by $\mathbb{D}^n_{>0}$ and $\mathbb{D}^n_+$.

2. Problem statement and preliminary results

Although in practice, the exact number of stages of parasitized erythrocytes is usually unknown, five main stages by simple morphology can be distinguished: young ring, old ring, trophozoite, early schizont and late schizont [5]. Hence, we reasonably assume that the parasitized erythrocytes population within the host is divided in 5 different stages: y_1, y_2, y_3, y_4 and y_5. The first two stages (y_1 and y_2) stand for the concentration of the free circulating parasitized erythrocytes and the last three stages correspond to the sequestered ones. The healthy cells x are generated with a constant recruitment Λ from the thymus and get infected by an effective contact with a merozoite m. During the late stage of infected cells, the erythrocyte ruptures and sets free r merozoites.

We assume that one can measure the concentration of circulating parasitaemia, *i.e.* $y_1 + y_2$. The main goal of this paper is to determine an estimate of the concentration of the sequestered parasitaemia, *i.e.* $y_3 + y_4 + y_5$. The following system is used to describe the dynamics of the parasitized erythrocytes $\forall t \geq 0$, [5, 6]:

$$
\begin{aligned}
\dot{z}(t) &= A(t)z(t) + E\beta(t)x(t)m(t) + e_1\Lambda(t), \\
Y(t) &= Cz(t) + v(t),
\end{aligned}
\tag{1}
$$

where $z = (x, y_1, \ldots, y_5, m)^{\mathrm{T}} \in \mathbb{R}^7_+$ is the state vector and $Y \in \mathbb{R}_+$ is the measured output, $v \in \mathcal{L}_\infty$ is the measurement noise, $||v||_\infty \leq V$ for some known $V > 0$; y_1 and y_2 represent the concentrations of free circulating erythrocytes and y_3, y_4, y_5 stand for the sequestered ones; x corresponds to the concentration of healthy cells, and m is the concentration of merozoites; $\Lambda(t) \in \mathbb{R}_+$, $\Lambda \in \mathcal{L}_\infty$ represents the recruitment of the healthy Red Blood Cells (RBC) and $\beta(t) \in \mathbb{R}_+$, $\beta \in \mathcal{L}_\infty$ is the rate of infection of RBC by merozoites. Note that in contrast to [5], we consider the practical and more realistic case in which the measurement output Y is corrupted by noise. The variables $\beta(t)$

and $\Lambda(t)$ serve as exogenous *uncertain* inputs in (1). We define the time-varying matrix $A(t)$ and the constant matrices C, E, e_1 as follows

$$C = [\ 0 \quad 1 \quad 1 \quad 0 \quad 0 \quad 0 \quad 0\ ],$$

$$E = [\ -1 \quad 1 \quad 0 \quad 0 \quad 0 \quad 0 \quad -1\ ]^{\mathrm{T}},$$

$$e_1 = [\ 1 \quad 0 \quad 0 \quad 0 \quad 0 \quad 0 \quad 0\ ]^{\mathrm{T}},$$

$$A(t) = \begin{bmatrix} -\mu_x & 0 & 0 & 0 & 0 & 0 & 0 \\ 0 & -\mu_1-\gamma_1 & 0 & 0 & 0 & 0 & 0 \\ 0 & \gamma_1 & -\mu_2-\gamma_2 & 0 & 0 & 0 & 0 \\ 0 & 0 & \gamma_2 & -\mu_3-\gamma_3 & 0 & 0 & 0 \\ 0 & 0 & 0 & \gamma_3 & -\mu_4-\gamma_4 & 0 & 0 \\ 0 & 0 & 0 & 0 & \gamma_4 & -\mu_5-\gamma_5 & 0 \\ 0 & 0 & 0 & 0 & 0 & r\gamma_5 & -\mu_m \end{bmatrix},$$

where $\mu_x > 0$ is the natural death rate of healthy cells; $\mu_i > 0$ is the natural death rate of ith stage of infected cells, $\gamma_i > 0$ represents the transition rate from i^{th} stage to $(i+1)^{\text{th}}$ stage of infected cells, $i = 1, \ldots, 5$; $r > 0$ correspond to the number of merozoites released by the late stage of infected cells, $\mu_m > 0$ stand for the natural death rate of merozoites.

The time-varying parameters μ_x, μ_i, γ_i, r and μ_x have different values for different patients and they vary with time for each patient. Therefore, we assume that the instant value of $A(t)$ is unavailable and

$$\underline{A} \le A(t) \le \overline{A} \ \forall t \ge 0$$

for some known Hurwitz and Metzler matrices $\underline{A}, \overline{A} \in \mathbb{R}^{7 \times 7}$ due to the structure of $A(t)$. Such a hypothesis is rather natural since on-line identification of these parameters is complicated and the shape of dependence of these parameters

on time is unknown. In a similar way, we assume that for the healthy RBC recruitment $\Lambda(t)$, the values $\underline{\Lambda}, \overline{\Lambda} \in \mathbb{R}_+$ are given such that

$$\underline{\Lambda} \leq \Lambda(t) \leq \overline{\Lambda} \; \forall t \geq 0.$$

Furthermore, we assume that for $\beta(t)$, there is no confidence interval since its instant value is highly uncertain in practice.

Moreover, we suppose that the measurement of the circulating *Plasmodium* concentration, *i.e.* $Y = y_1 + y_2 + v$ is obtained with a noise v, while estimation of the sequestered one $Z = y_3 + y_4 + y_5$ is required. We need the following assumption in the sequel to ensure nonnegativity and boundedness for the state vector $z(t)$ of (1) since it represents concentrations.

Assumption 1. *The state $z(t)$ of (1) is nonnegative and is bounded $(z(t) \in \mathcal{L}_\infty^7)$ for all $t \geq 0$.*

The goal of this article is to design an interval observer, *i.e.*, state signal bounds $0 \leq \underline{z}(t) \leq z(t) \leq \overline{z}(t)$, for all $t \geq 0$, in order to estimate $Z(t)$. We aim to design this interval observer such that the interval $\overline{z}(t) - \underline{z}(t)$ is as tight as possible to obtain an accurate state estimation.

3. Interval observer design

In this section, we design an interval estimator for the patient's model (1). We assume that neither $\beta(t)$ nor its bounding values are available, which makes the estimation problem more challenging but more realistic [5, 23, 6]. First, we determine upper and lower bounds for an auxiliary uncertain input for (1). Next, we design an interval observer for the model (1) providing a lower $\underline{z}(t)$ and an upper $\overline{z}(t)$ bounds for $z(t)$. We prove the inclusion relation $0 \leq \underline{z}(t) \leq z(t) \leq \overline{z}(t)$, $\quad \forall t \geq 0$. Finally, we evaluate bounds for $\beta(t)$.

Define an auxiliary uncertain input for (1):

$$w(t) = \beta(t)x(t)m(t),$$

which is a new unmeasurable variable. By using the equation (1), we deduce that

$$w(t) = ((CE)^{\mathrm{T}}CE)^{-1}(CE)^{\mathrm{T}}(C\dot{z}(t) - CA(t)z(t) - Ce_1\Lambda(t)),$$

where $C\dot{z}$ is proportional to the derivative of the output $\dot{Y}$. By using the structure of the patient's model (1), one can notice that $CE = 1$. To design lower

and upper bounds for the uncertain input w, we need to estimate the derivative $\dot{z}$. For this purpose, we will use the following non-homogenous sliding mode differentiator: consider a measured signal $\tilde{y}(t) = y(t) + \nu(t)$, where $y : \mathbb{R}_+ \to \mathbb{R}$ is a signal to be differentiated and $\nu \in \mathcal{L}_\infty$ represents a bounded measurement noise, then a differentiation algorithm can be formulated in the form

$$\dot{x}_1 = -\alpha\sqrt{|x_1 - \tilde{y}(t)|}\text{sign}(x_1 - \tilde{y}(t)) + x_2, \qquad (2)$$
$$\dot{x}_2 = -\varrho\,\text{sign}(x_1 - \tilde{y}(t)) - \chi\,\text{sign}(x_2) - x_2,$$
$$x_1(0) = \tilde{y}(0), \ x_2(0) = 0,$$

where $x_1, x_2 \in \mathbb{R}$ represent the state variables of the system (2), α, ϱ and χ are the tuning parameters with $\alpha > 0$ and $\varrho > \chi \geq 0$. The variable $x_1(t)$ stands for an estimate of the function $y(t)$, and $x_2(t)$ corresponds to an estimate of $\dot{y}(t)$. Hence, the system (2) has $\tilde{y}(t)$ as the input and $\hat{y}(t) = x_2(t)$ as the output.

Lemma 1. [25] *Let $\dot{y}, \ddot{y}, \nu \in \mathcal{L}_\infty$. There exist $\alpha > 0$ and $\varrho > \chi \geq 0$ such that $x_1, x_2 \in \mathcal{L}_\infty$ and there exist $T_0 > 0$, $c_1 > 0$ and $c_2 > 0$*

$$|x_2(t) - \dot{y}(t)| \leq \sqrt{c_1||\nu||_\infty + \sqrt{c_2||\nu||_\infty}} \quad \forall t \geq T_0.$$

For information on estimates on $T_0 > 0$, $c_1 > 0$, $c_2 > 0$ and guidelines for tuning α, ϱ, χ , we refer an interested reader to [25].

Remark 1. *The differentiator (2) provides us essentially with an on-line estimate of the derivative of a noisy signal. The advantages of the differentiator (2) consist in its simplicity of evaluation of the estimation error convergence time, accuracy of derivative calculation and robustness against a non-differentiable noise of any amplitude (the Lyapunov function method was used to achieve these goals in [25]). These advantages are very useful, especially for numerical simulations with non-differentiable noise (see Section 5).*

By applying Lemma 1 and the differentiator (2), we determine an estimate $\hat{\dot{Y}}$ of $C\dot{z}$ (or $\dot{Y}$) such that for all $t \geq 0$

$$\dot{Y}(t) = \hat{\dot{Y}}(t) + v'(t),$$

where $v' \in \mathbb{R}$ represents an error of differentiation of the noisy output Y, and $||v'||_\infty < V'$ for some known $V' > 0$ according to Lemma 1 (v' can be viewed as a kind of measurement noise for $\dot{Y}$).

Next, we review some basic facts about interval estimation and positive systems, which are needed in the following.

Lemma 2. [17] *Let $x \in \mathbb{R}^n$ be a vector variable, $\underline{x} \leq x \leq \overline{x}$ for some $\underline{x}, \overline{x} \in \mathbb{R}^n$. If $A \in \mathbb{R}^{m \times n}$ is a constant matrix, then*

$$A^+ \underline{x} - A^- \overline{x} \leq Ax \leq A^+ \overline{x} - A^- \underline{x}. \tag{3}$$

(2) If $A \in \mathbb{R}^{m \times n}$ is a matrix variable and $\underline{A} \leq A \leq \overline{A}$ for some $\underline{A}, \overline{A} \in \mathbb{R}^{m \times n}$, then

$$\underline{A}^+ \underline{x}^+ - \overline{A}^+ \underline{x}^- - \underline{A}^- \overline{x}^+ + \overline{A}^- \overline{x}^- \leq Ax \tag{4}$$
$$\leq \overline{A}^+ \overline{x}^+ - \underline{A}^+ \overline{x}^- - \overline{A}^- \underline{x}^+ + \underline{A}^- \underline{x}^-.$$

Moreover, if $-\overline{A} = \underline{A} \leq 0 \leq \overline{A}$, then one can simplify the inequality (4) as $-\overline{A}(\overline{x}^+ + \underline{x}^-) \leq Ax \leq \overline{A}(\overline{x}^+ + \underline{x}^-)$.

Lemma 3. [26, 27] *Consider the following linear time-invariant (LTI) system*

$$\begin{aligned} \dot{x} &= \mathcal{A}x + B\omega(t), \ \omega : \mathbb{R}_+ \to \mathbb{R}_+^q, \\ y &= Cx + D\omega(t), \end{aligned} \tag{5}$$

where $x \in \mathbb{R}^n$, $y \in \mathbb{R}^p$ and the matrix $\mathcal{A} \in \mathbb{R}^{n \times n}$ is Metzler. Any solution of the LTI system (5) is elementwise nonnegative for all $t \geq 0$ provided that $x(0) \geq 0$ and $B \in \mathbb{R}_+^{n \times q}$. Also, the output solution $y(t)$ of such a system is nonnegative if $C \in \mathbb{R}_+^{p \times n}$ and $D \in \mathbb{R}_+^{p \times q}$. A dynamical system satisfying all these restrictions is called cooperative (monotone) or nonnegative.

For the patient's model (1), assume that the estimates $\underline{z}(t)$ and $\overline{z}(t)$ are available such that $0 \leq \underline{z}(t) \leq z(t) \leq \overline{z}(t)$ for all $t \geq 0$. By applying Lemma 2, since the matrix C is nonnegative, we obtain the following relations for $t \geq 0$:

$$\underline{w}(t) \leq w(t) \leq \overline{w}(t), \tag{6}$$

where $\underline{w} = \hat{Y} - V' - Ce_1\overline{\Lambda} - (C\overline{A})^+ \overline{z} + (C\overline{A})^- \underline{z}$ and $\overline{w} = \hat{Y} + V' - Ce_1\underline{\Lambda} - (C\underline{A})^+ \underline{z} + (C\underline{A})^- \overline{z}$.

Then an interval observer equations for (1) take the form

$$
\begin{aligned}
\dot{\underline{\zeta}}(t) &= \underline{A}\underline{\zeta}(t) + e_1\underline{\Lambda} + E^+\underline{w}(t) \\
&\quad - E^-\overline{w}(t) + \underline{L}(Y(t) - C\underline{\zeta}(t)) - |\underline{L}|V, \\
\dot{\overline{\zeta}}(t) &= \overline{A}\overline{\zeta}(t) + e_1\overline{\Lambda} + E^+\overline{w}(t) \\
&\quad - E^-\underline{w}(t) + \overline{L}(Y(t) - C\overline{\zeta}(t)) + |\overline{L}|V, \\
\underline{z}(t) &= \max\{0, \underline{\zeta}(t)\}, \\
\overline{z}(t) &= \max\{0, \overline{\zeta}(t)\},
\end{aligned}
\tag{7}
$$

where $\underline{z} \in \mathbb{R}^7$ and $\overline{z} \in \mathbb{R}^7$ represent respectively the lower and the upper interval estimates for the state z; $\underline{\zeta}, \overline{\zeta} \in \mathbb{R}^7$ is the state of (7).

We select the observer gains $\overline{L} \in \mathbb{R}^{7\times1}$, $\underline{L} \in \mathbb{R}^{7\times1}$ such that the matrices $\overline{A} - \overline{L}C$ and $\underline{A} - \underline{L}C$ are Hurwitz and Metzler, to ensure positivity and asymptotic stability for the error dynamics (Lemma 3). Observer gains that satisfy such conditions exist since the matrices $\underline{A}$ and $\overline{A}$ are Hurwitz and Metzler by construction (for example $\overline{L} = \underline{L} = 0$ is an admissible choice).

Theorem 1. *Let the Assumption 1 be satisfied. The estimates $\underline{z}(t)$ and $\overline{z}(t)$ given by (7) yield the relations*

$$
0 \le \underline{z}(t) \le z(t) \le \overline{z}(t) \quad \forall t \ge 0 \tag{8}
$$

for all $t \in \mathbb{R}_+$ provided that $0 \le \underline{z}(0) \le z(0) \le \overline{z}(0)$.

Proof. We rewrite the equation (1) as follows

$$
\dot{z} = (A' - LC)z + (A(t) - A')z + Ew + e_1\Lambda + LY - Lv
$$

for some $A' \in \mathbb{R}^{7\times7}$ ($\underline{A}$ or $\overline{A}$) and $L \in \mathbb{R}^{7\times1}$ ($\underline{L}$ or $\overline{L}$). Define the errors $\underline{e}(t) = z(t) - \underline{\zeta}(t)$, $\overline{e}(t) = \overline{\zeta}(t) - z(t)$, then the error dynamics obey the equations

$$
\begin{aligned}
\dot{\underline{e}}(t) &= (\underline{A} - \underline{L}C)\underline{e}(t) + \underline{g}(t), \\
\dot{\overline{e}}(t) &= (\overline{A} - \overline{L}C)\overline{e}(t) + \overline{g}(t),
\end{aligned}
\tag{9}
$$

where

$$\underline{g} = (A(t) - \underline{A})z + Ew - E^+\underline{w} + E^-\overline{w}$$
$$+ e_1(\Lambda - \underline{\Lambda}) - \underline{L}v + |\underline{L}|V,$$
$$\overline{g} = (\overline{A} - A(t))z + E^+\overline{w} - E^-\underline{w} - Ew$$
$$+ e_1(\overline{\Lambda} - \Lambda) + \overline{L}v + |\overline{L}|V.$$

By applying Lemma 2, we conclude that $\underline{g}(t) \geq 0$, $\overline{g}(t) \geq 0$ $\forall t \geq 0$. Since the matrices $\overline{A} - \overline{L}C$ and $\underline{A} - \underline{L}C$ are Metzler, we deduce by applying the Lemma 3 that $\underline{e}(t) \geq 0$ and $\overline{e}(t) \geq 0$ since $\underline{e}(0) \geq 0$ and $\overline{e}(0) \geq 0$ (the system (9) is cooperative). Consequently, the order relation $\underline{\zeta}(t) \leq z(t) \leq \overline{\zeta}(t)$ is satisfied for all $t \geq 0$. Hence (8) is true by construction of $\underline{z}, \overline{z}$. $\qquad \square$

The obtained interval estimates $\underline{z}, \overline{z}$ are nonnegative as the state z is. To conclude this section, recall that apart from [5], estimation approaches in the existing literature assume that the value of the infection rate parameter β is known, whereas this parameter is highly uncertain in practice. To circumvent this issue, our interval observer (7) does not impose such an assumption. Moreover, we use an estimation method that allows lower and upper bounds of β to be evaluated when $\underline{xm} \neq 0$ (and then $\overline{xm} \neq 0$). We deduce from (6) that for all $t \geq 0$

$$\underline{\beta}(t) \leq \beta(t) \leq \overline{\beta}(t), \tag{10}$$

with

$$\underline{\beta} = (\overline{xm})^{-1}(\hat{Y} - V' - Ce_1\overline{\Lambda}$$
$$- (C\overline{A})^+\overline{z} + (C\overline{A})^-\underline{z}),$$
$$\overline{\beta} = (\underline{xm})^{-1}(\hat{Y} + V' - Ce_1\underline{\Lambda}$$
$$- (C\underline{A})^+\underline{z} + (C\underline{A})^-\overline{z}).$$

Notice that when $\underline{xm}$ is close to 0 (and then $\overline{xm}$ is close to 0), the estimates $\underline{\beta}$ and $\overline{\beta}$ become conservative.

Assumption 1 implies that the state vector z is a finite vector ($z \in \mathcal{L}_\infty^7$). Next, we introduce conditions that are efficiently computable by using linear programming and under which the interval observer is stable, *i.e.*, the estimates $\underline{z}, \overline{z} \in \mathcal{L}_\infty^7$.

4. Computational considerations

The result of Theorem 1 does not indicate a way how the corresponding observer gains $\underline{L}$, $\overline{L}$ can be computed to ensure boundedness for $\underline{z}, \overline{z}$. Hence, we need to develop an efficient method to solve this issue. We aim at computing observer gains that minimize the estimation errors $z - \underline{z}$ and $\overline{z} - z$.

Our approach consists in computing the observer gains $\underline{L}$, $\overline{L}$ as solutions of an optimization problem of the L_∞ gain of the interval estimation error dynamics [28]. For this purpose, let us introduce upper $\underline{Z}(t)$ and lower $\overline{Z}(t)$ estimates for the variable of interest $Z(t)$:

$$\underline{Z}(t) = \sum_{i=4}^{6} \underline{\zeta}_i(t), \ \overline{Z}(t) = \sum_{i=4}^{6} \overline{\zeta}_i(t),$$

and the corresponding estimation errors

$$\underline{\epsilon}(t) = Z(t) - \underline{Z}(t) = \sum_{i=4}^{6} e_i(t),$$

$$\overline{\epsilon}(t) = \overline{Z}(t) - Z(t) = \sum_{i=4}^{6} \overline{e}_i(t).$$

Considering $\underline{\epsilon}(t)$, $\overline{\epsilon}(t)$ as the outputs for the error system (9) we can rewrite it as follows

$$
\begin{aligned}
\dot{\underline{e}}(t) &= (\underline{A} - \underline{L}C)\underline{e}(t) + \underline{\omega}(t) + \underline{L}^+(V - v) + \underline{L}^-(V + v), \\
\underline{\epsilon}(t) &= \Theta\underline{e}(t), \quad\quad\quad\quad\quad\quad\quad\quad\quad\quad\quad\quad\quad\quad (11) \\
\dot{\overline{e}}(t) &= (\overline{A} - \overline{L}C)\overline{e}(t) + \overline{\omega}(t) + \overline{L}^+(V + v) + \overline{L}^-(V - v), \\
\overline{\epsilon}(t) &= \Theta\overline{e}(t), \quad\quad\quad\quad\quad\quad\quad\quad\quad\quad\quad\quad\quad\quad (12)
\end{aligned}
$$

where

$$
\begin{aligned}
\Theta &= [0\,0\,0\,1\,1\,1\,0], \\
\underline{\omega} &= (A(t) - \underline{A})z + Ew - E^+\underline{w} \\
&\quad + E^-\overline{w} + e_1(\Lambda - \underline{\Lambda}), \\
\overline{\omega} &= (\overline{A} - A(t))z + E^+\overline{w} - E^-\underline{w} \\
&\quad - Ew + e_1(\overline{\Lambda} - \Lambda).
\end{aligned}
$$

Define

$$\varsigma = \begin{bmatrix} \underline{\omega} \\ V - v \\ V + v \end{bmatrix}, \bar{\varsigma} = \begin{bmatrix} \overline{\omega} \\ V + v \\ V - v \end{bmatrix}.$$

We aim at selecting observer gains $\underline{L}, \overline{L}$ that minimize the L_∞ gain (peak-to-peak gain) from ς to $\underline{\epsilon}$ in (11) and from $\bar{\varsigma}$ to $\bar{\epsilon}$ in (12). Notice that these systems are nonnegative since the matrices $\overline{A} - \overline{L}C$ and $\underline{A} - \underline{L}C$ are Metzler (Lemma 3).

First, we review some basic facts and definitions about the L_∞ gain of nonnegative systems [29, 30, 28]. We denote the output signal of the system (5) with the initial condition $x(0) = 0$ and the input ω as $y := \mathcal{G}\omega$, where $\mathcal{G}(s) = C(sI_n - \mathcal{A})^{-1}B$ is the corresponding transfer function.

Definition 1. For the system (5), its input-output L_∞ gain is defined as $\sup_{\|\omega\|_\infty = 1} \|\mathcal{G}\omega\|_\infty$.

The next result presents a way for efficient evaluation of this gain:

Theorem 2. [28] *Let the matrix $\mathcal{A} \in \mathbb{R}^{n \times n}$ be Metzler and $B \in \mathbb{R}_+^{n \times q}$, $C \in \mathbb{R}_+^{p \times n}$, $D \in \mathbb{R}_+^{p \times q}$. For a scalar $\gamma > 0$ the following statements are equivalent:*

(a) The nonnegative LTI system (5) is asymptotically stable for $\omega = 0$ and its L_∞ gain is strictly less than γ.

(b) The following Linear Program (LP) is feasible:

$$\text{There exists } \lambda \in \mathbb{R}_{>0}^n \text{ such that } \begin{bmatrix} \mathcal{A}\lambda + B\mathbb{1}_q \\ C\lambda - \gamma\mathbb{1}_p + D\mathbb{1}_q \end{bmatrix} < 0. \tag{13}$$

Theorem 2 constitutes the basis for the optimization of the interval observer gains $\underline{L}, \overline{L}$ using linear programming, as developed in Proposition 1 below. Notwithstanding that one can derive this proposition by using arguments from Theorem 14 in [28], we provide direct proofs in this article for clarity and completeness of exposition. To this end the following theorem about stability of Metzler matrices is needed:

Theorem 3. [26] *Let a matrix $A \in \mathbb{R}^{n \times n}$ be Metzler. The following statements are equivalent:*

(a) The matrix A is Hurwitz.

(b) There exists $h \in \mathbb{R}_{>0}^n$ such that $Ah < 0$.

(c) There exists $h \in \mathbb{R}_{>0}^n$ such that $h^T A < 0$.

Next, we derive a more suitable version of the LP (13) for the scenario in which $D = 0$ and the system (5) has a single output by using Theorem 3:

Theorem 4. *Consider the system (5) and let the matrix $\mathcal{A} \in \mathbb{R}^{n \times n}$ be Metzler and $B \in \mathbb{R}_+^{n \times q}$, $C \in \mathbb{R}_+^{1 \times n}$, $D = 0$. For a scalar $\gamma > 0$ the following statements are equivalent:*

(a) The nonnegative LTI system (5) is asymptotically stable and its L_∞ gain is strictly less than γ.

(b) The following Linear Program (LP) is feasible:

$$\text{There exists } \Omega \in \mathbb{D}_{>0}^n \text{ such that } \mathbb{1}_{n+1}^T \begin{bmatrix} \Omega \mathcal{A} & \Omega B \mathbb{1}_q \\ C & -\gamma \end{bmatrix} < 0. \tag{14}$$

Proof. For the case in which $D = 0$ and $p = 1$, the LP (13) is equivalent to

$$\text{There exists } \lambda \in \mathbb{R}_{>0}^n \text{ such that } \begin{bmatrix} \mathcal{A} & B \mathbb{1}_q \\ C & -\gamma \end{bmatrix} \begin{bmatrix} \lambda \\ 1 \end{bmatrix} < 0. \tag{15}$$

One can remark that in (15), the matrix in the left-hand side is Metzler since $\mathcal{A} \in \mathbb{R}^{n \times n}$ is Metzler, $B \in \mathbb{R}_+^{n \times q}$ and $C \in \mathbb{R}_+^{1 \times n}$. We deduce by applying Theorem 3 that the LP (15) can be replaced by

$$\text{There exists } \varsigma \in \mathbb{R}_{>0}^{n+1} \text{ such that } \varsigma^T \begin{bmatrix} \mathcal{A} & B \mathbb{1}_q \\ C & -\gamma \end{bmatrix} < 0.$$

Then, the following LP can be obtained by normalizing the vector ς

$$\text{There exists } \kappa \in \mathbb{R}_{>0}^n \text{ such that } \begin{bmatrix} \kappa \\ 1 \end{bmatrix}^T \begin{bmatrix} \mathcal{A} & B \mathbb{1}_q \\ C & -\gamma \end{bmatrix} < 0. \tag{16}$$

By using the identity

$$\begin{bmatrix} \kappa \\ 1 \end{bmatrix}^T = \mathbb{1}_{n+1}^T \begin{bmatrix} \Omega & 0 \\ 0 & 1 \end{bmatrix},$$

while writing $\kappa = \Omega \mathbb{1}_n$ with $\Omega = \text{diag}\{\kappa\}$, the result (14) can be deduced directly from (16). $\square$

Next, we solve the problem of selecting the observer gains $\underline{L}, \overline{L}$ that minimize the L_∞ gains of the estimation errors dynamics. First, we derive the following

14

proposition.

Proposition 1. *Let the Assumption 1 be satisfied and the matrices $(\underline{A} - \underline{L}C)$ and $(\overline{A} - \overline{L}C)$ be Metzler. The L_∞ gain of the system (11) with input $\underline{\varsigma}$ and output $\underline{\epsilon}$ is smaller than $\underline{\gamma} > 0$ if there exists $\underline{\Omega} \in \mathbb{D}^7_{>0}$ such that*

$$\mathbb{1}_8^T \begin{bmatrix} \underline{\Omega}(\underline{A} - (\underline{L}^+ - \underline{L}^-)C) & \underline{\Omega}\Pi_1 \\ \Theta & -\underline{\gamma} \end{bmatrix} < 0,$$
$$\Pi_1 = \mathbb{1}_7 + \underline{L}^+ + \underline{L}^-. \tag{17}$$

The L_∞ gain of the system (12) with input $\overline{\varsigma}$ and output $\overline{\epsilon}$ is smaller than $\overline{\gamma} > 0$ if there exists $\overline{\Omega} \in \mathbb{D}^7_{>0}$ such that

$$\mathbb{1}_8^T \begin{bmatrix} \overline{\Omega}(\overline{A} - (\overline{L}^+ - \overline{L}^-)C) & \overline{\Omega}\Pi_2 \\ \Theta & -\overline{\gamma} \end{bmatrix} < 0,$$
$$\Pi_2 = \mathbb{1}_7 + \overline{L}^+ + \overline{L}^-. \tag{18}$$

Moreover, when the conditions (17)–(18) occur, $\underline{\varsigma}, \overline{\varsigma} \in \mathcal{L}^7_\infty$ and so $\underline{z}, \overline{z} \in \mathcal{L}^7_\infty$ provided that

$$\underline{\gamma} < \frac{1}{\|E^+(C\overline{A})^- + E^-(C\underline{A})^+\|}, \quad \overline{\gamma} < \frac{1}{\|E^+(C\underline{A})^- + E^-(C\overline{A})^+\|},$$
$$\underline{\gamma}\overline{\gamma} < \frac{1}{\|E^-(C\underline{A})^- + E^+(C\overline{A})^+\|\|E^+(C\underline{A})^+ + E^-(C\overline{A})^-\|}.$$

Proof. By definition, we get $\underline{L} = \underline{L}^+ - \underline{L}^-$ and $\overline{L} = \overline{L}^+ - \overline{L}^-$. Since the error systems (11) and (12) are nonnegative, one can deduce the following LPs directly by using (14):

$$\mathbb{1}_8^T \begin{bmatrix} \underline{\Omega}(\underline{A} - (\underline{L}^+ - \underline{L}^-)C) & \underline{\Omega}B_1 \begin{bmatrix} \mathbb{1}_7 \\ 1 \\ 1 \end{bmatrix} \\ \Theta & -\underline{\gamma} \end{bmatrix} < 0,$$
$$B_1 = \begin{bmatrix} I_7 & \underline{L}^+ & \underline{L}^- \end{bmatrix},$$

15

and

$$
\mathbb{1}_8^{\mathrm{T}} \begin{bmatrix} \overline{\Omega}(\overline{A} - (\overline{L}^+ - \overline{L}^-)C) & \overline{\Omega} B_2 \begin{bmatrix} \mathbb{1}_7 \\ 1 \\ 1 \end{bmatrix} \\ \Theta & -\overline{\gamma} \end{bmatrix} < 0,
$$

$$
B_2 = \begin{bmatrix} I_7 & \overline{L}^+ & \overline{L}^- \end{bmatrix}.
$$

Furthermore, it can be inferred from Theorem 2 that the internal error dynamics (11) and (12) are stable, and the small-gain conditions imposed on $\underline{\gamma}$ and $\overline{\gamma}$ take into account the nonlinearities appeared in $\underline{\omega}$ and $\overline{\omega}$, which implies that $\underline{e}, \overline{e} \in \mathcal{L}_\infty^7$. We conclude that $\underline{\zeta}, \overline{\zeta} \in \mathcal{L}_\infty^7$ since $z \in \mathcal{L}_\infty^7$ by Assumption 1. It can be inferred that $\underline{z}, \overline{z} \in \mathcal{L}_\infty^7$. $\qquad\square$

The next theorem optimizes the interval observer gains $\underline{L}, \overline{L}$:

Theorem 5. *Consider the following optimization problems under linear inequalities constraints with respect to $\underline{\Omega}, \overline{\Omega} \in \mathbb{D}_{>0}^7$, $U_1, U_2, U_3, U_4 \in \mathbb{R}_+^{7\times 1}$, $\underline{\gamma}, \overline{\gamma} \in \mathbb{R}_+$ and auxiliary diagonal matrices $\Gamma_1, \Gamma_2 \in \mathbb{D}_+^7$*

$$
\inf_{\underline{\gamma}, \underline{\Omega}, U_1, U_2, \Gamma_1} \underline{\gamma}, \tag{19}
$$

$$
s.t. \; \mathbb{1}_8^T \begin{bmatrix} \underline{\Omega}\,\underline{A} - (U_1 - U_2)C & \Psi_1 \\ \Theta & -\underline{\gamma} \end{bmatrix} < 0, \tag{20}
$$

$$
\Psi_1 = U_1 + U_2 + \underline{\Omega}\mathbb{1}_7, \tag{21}
$$

$$
\underline{\Omega}\,\underline{A} - (U_1 - U_2)C + \Gamma_1 > 0, \tag{22}
$$

$$
\underline{\gamma} > 0, U_1, U_2 > 0, \tag{23}
$$

$$
\underline{\Omega}\mathbb{1}_7 > 0, \Gamma_1 \mathbb{1}_7 \geq 0, \tag{24}
$$

and

$$\inf_{\overline{\gamma}, \overline{\Omega}, U_3, U_4, \Gamma_2} \overline{\gamma}, \tag{25}$$

$$s.t. \mathbb{1}_8^T \begin{bmatrix} \overline{\Omega}\,\overline{A} - (U_3 - U_4)C & \Psi_2 \\ \Theta & -\overline{\gamma} \end{bmatrix} < 0, \tag{26}$$

$$\Psi_2 = U_3 + U_4 + \overline{\Omega}\mathbb{1}_7, \tag{27}$$

$$\overline{\Omega}\,\overline{A} - (U_3 - U_4)C + \Gamma_2 > 0, \tag{28}$$

$$\overline{\gamma} > 0, U_3, U_4 > 0, \tag{29}$$

$$\overline{\Omega}\mathbb{1}_7 > 0, \Gamma_2\mathbb{1}_7 \geq 0. \tag{30}$$

Then, we can compute the optimal gains $\underline{L}, \overline{L}$ for the interval observer (7) as follows

$$\underline{L}^\star = (\underline{\Omega}^\star)^{-1}(U_1^\star - U_2^\star),$$
$$\overline{L}^\star = (\overline{\Omega}^\star)^{-1}(U_3^\star - U_4^\star),$$

where $\underline{\Omega}^\star, U_1^\star$ and $U_2^\star$ are optimal solutions of the problem (19)–(24) and $\overline{\Omega}^\star, U_3^\star$ and $U_4^\star$ are optimal solutions of the problem (25)–(30).

Proof. We obtain the linear inequalities (20) and (26) by substituting

$$U_1 = \underline{\Omega}L^+, U_2 = \underline{\Omega}L^-, U_3 = \overline{\Omega}L^+, U_4 = \overline{\Omega}L^-$$

in (17)-(18). The constraints (22) and (28) are equivalent to say that the matrices $(\underline{A} - \underline{L}C)$ and $(\overline{A} - \overline{L}C)$ are Metzler, while the constraints (24) and (30) are equivalent to say that $\underline{\Omega} \in \mathbb{D}_{>0}^7, \Gamma_1 \in \mathbb{D}_+^7$ and $\overline{\Omega} \in \mathbb{D}_{>0}^7, \Gamma_2 \in \mathbb{D}_+^7$. $\qquad\square$

Note that the optimization problems (19)–(24) and (25)–(30) can be easily solved with standard linear programming solvers.

Next, we demonstrate efficiency of the proposed interval observer and the tuning procedure in simulation and using a real data.

5. Simulation of the interval observer

In this section, first, the result of numerical simulations are reported for the model (1). Next, we validate the efficiency of the approach by using real data measured for an infected patient.

17

Parameters of the matrix $A(t)$ have the following constant values for patients without fever, *i.e.* at 37°C as in [5]:

$$\gamma_1 = 1.96, \gamma_2 = 3.78, \gamma_3 = 2.85, \gamma_4 = 1.76, \gamma_5 = 3.26;$$

$$\mu_1 = 0, \mu_2 = 1.86, \mu_3 = 0, \mu_4 = 0.1, \mu_5 = 0; \tag{31}$$

$$\mu_x = \frac{1}{120}, r = 16, \mu_m = 72.$$

Consider the case in which admissible deviations of these parameters from the nominal values are given above $\sigma\%$ (where σ is an adjusted parameter). Therefore, we determine the matrices $\underline{A}$ and $\overline{A}$. The healthy RBC recruitment's nominal value is $\Lambda_0 = \frac{5 \times 10^6}{120}$ cellsμl^{-1}day^{-1} (as in [5], the volume unit considered is micro-liter (μl) and the time unit is day) with admissible deviations $\pm 20\%$, *i.e.*

$$0.8\Lambda_0 = \underline{\Lambda} \leq \Lambda(t) \leq \overline{\Lambda} = 1.2\Lambda_0 \ \forall t \geq 0.$$

For an abstract model simulations, we use the following values

$$\Lambda(t) = \text{rand}(0.8\Lambda_0, 1.2\Lambda_0)$$
$$\beta(t) = 10^{-6}(1 + 0.25\sin(5t))e^{\text{mod}^2(t, 2.5 + 0.5\sin(0.25t))},$$
$$v(t) = \text{rand}(-V, V), \ V = 100, \tag{32}$$
$$A(t) = \sin^2(3t)\underline{A} + \cos^2(3t)\overline{A},$$

where $\text{rand}(a, b)$ provides us with independent random numbers that follows a continuous uniform distribution over the interval $[a, b]$. Let $\underline{z}(0) = \frac{1}{3}\overline{z}(0) = [500 \ 100 \ 150 \ 50 \ 50 \ 50 \ 50]^{\text{T}}$ and $z(0) = 2\underline{z}(0)$. For the differentiator (2), we select $\alpha = 2 \times 10^3$, $\varrho = 3\alpha$ and $\chi = 0.25\alpha$, $V' = 80V$, and the sampling period is the same as the measurement period for simulations. To solve the optimization problems of Theorem 5, we use Matlab YALMIP toolbox [31] with the solver MOSEK.

Let us perform simulations with some values of σ to test the accuracy and robustness of our interval observer (7). When $\sigma = 5$, *i.e.*, in the case in which parameters of the matrix $A(t)$ deviate from their nominal values by 5%, using

Theorem 5, we obtain the optimal interval observer gains

$$\underline{L}^\star = [0\ 0\ 1.862\ 0\ 0\ 0\ 0]^{\mathrm{T}},$$
$$\overline{L}^\star = [0\ 0\ 2.058\ 0\ 0\ 0\ 0]^{\mathrm{T}}.$$

When $\sigma = 10$, we obtain the optimal interval observer gains

$$\underline{L}^\star = [0\ 0\ 1.764\ 0\ 0\ 0\ 0]^{\mathrm{T}},$$
$$\overline{L}^\star = [0\ 0\ 2.156\ 0\ 0\ 0\ 0]^{\mathrm{T}}.$$

Finally, when $\sigma = 20$, we obtain the optimal interval observer gains

$$\underline{L}^\star = [0\ 0\ 1.568\ 0\ 0\ 0\ 0]^{\mathrm{T}},$$
$$\overline{L}^\star = [0\ 0\ 2.352\ 0\ 0\ 0\ 0]^{\mathrm{T}}.$$

By visualizing the results of interval estimation for sequestered *Plasmodium* $Z = y_3 + y_4 + y_5$ for $\sigma = 5, \sigma = 10$ and $\sigma = 20$, we deduce that the inclusion relation (8) is satisfied when using our interval observer, and the size of uncertainty σ influences directly the estimation accuracy (Fig.1).

5.2. Real data simulations

In this subsection, the measured concentration of circulating parasites (peripheral *parasitaemia*, which consists of parasites density in the blood) consists of data collected by the US Public Health Service at the National Institutes of Health laboratories in Columbia, South Carolina and Milledgeville, Georgia [32, 33], where malaria was used for therapy of neurosyphilis, and patients were inoculated through mosquito bite or infected blood (see also [5] for more details). We use the data of the patient named S1204 for simulations (Fig.2). We select the same parameters for the model as in [5]. For the parameters $\Lambda(t)$, $\beta(t)$ and $v(t)$, we use the same formulas as in (32), with $V = 7500$.

For the differentiator (2), we select $\chi = 1000$, $\alpha = 4(2\sqrt{2}\chi + \sqrt{\chi})$, $\varrho = 2.7 \times 10^8 + 2\chi$ and $V' = 9V$. We perform the simulations with the same values of deviation $\sigma\%$ as in Subsection 5.1. By visualizing the results of interval estimation, we notice that the inclusion relation (8) is satisfied when using our interval observer with the real data of the patient S1204. Furthermore, as in Subsection 5.1, we remark that the size of uncertainty σ has a direct impact on the estimation accuracy (Fig. 3).
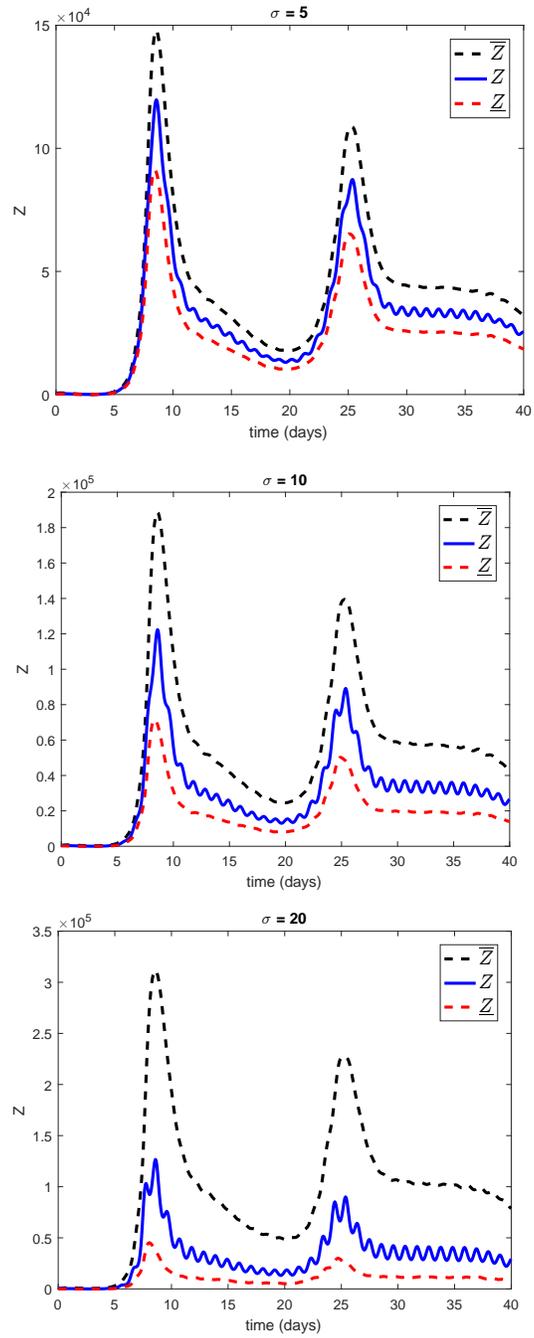
Figure 1: Results of interval estimation for sequestered parasites
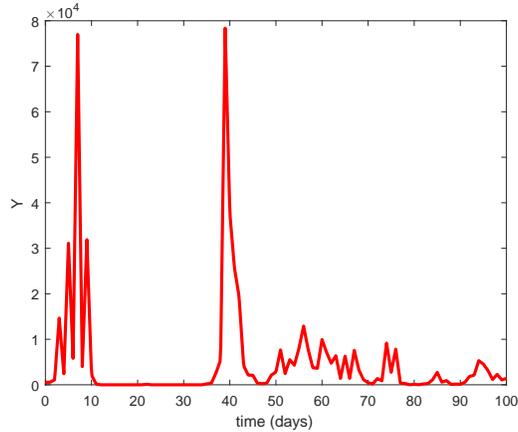
Figure 2:   Patient S1204: Measurements (data) $Y(t)$

6. Conclusion

This article solves the problem of sequestered erythrocytes estimation from the measured circulating parasites in malaria patients. We have designed an interval observer that provides intervals of admissible values for the sequestered parasite population. We have assumed that almost all parameters and inputs of the model are uncertain (just intervals of admissible values are given except for infection rates, whose bounding values are unavailable) and we have considered noisy measurements. Despite of that, the proposed observer demonstrates a reasonable accuracy of interval estimation. Furthermore, we have designed an algorithm for optimization of the corresponding interval observer L_∞ gains from the uncertain signals to the estimated quantities. We demonstrated the efficiency of the proposed approach by numerical simulations for a theoretical model and for real measured data. Future research can extend the methodology to a scenario with discrete-time measurement output and continuous-time model, following the approach proposed in [34]. Another direction to consider for future work could consist in a joint estimation of the state x and the unknown input w.

Acknowledgement
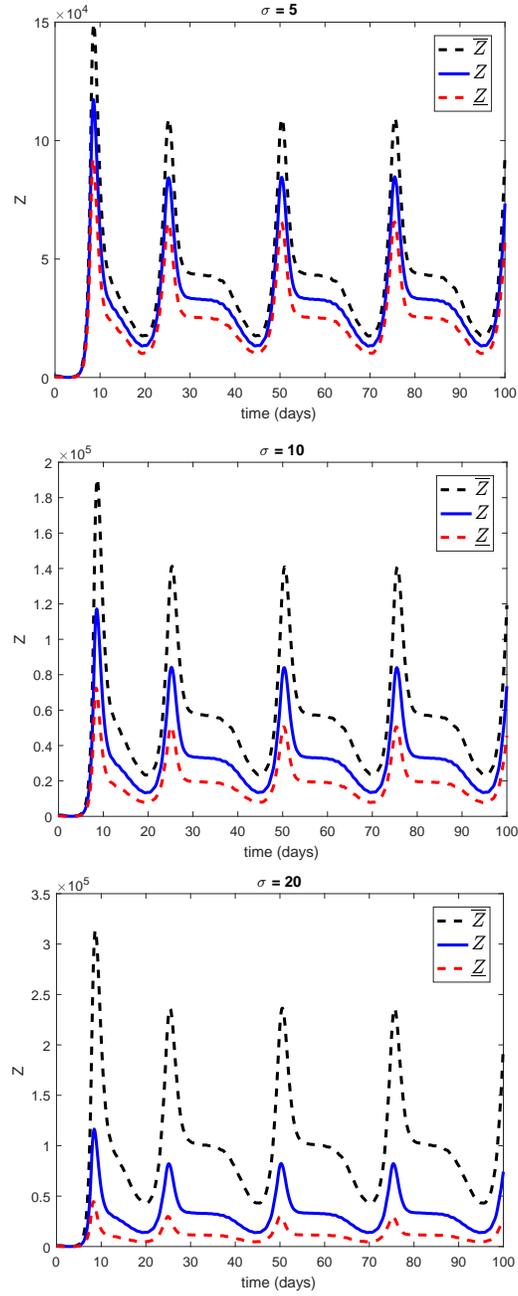
Figure 3: Patient S1204: Results of interval estimation for sequestered parasites

22

References

[1] The World Malaria Report 2019 at glance, Tech. rep., World Health Organization (WHO), Geneva, Switzerland (Dec. 2019).

[2] M. B. Gravenor, A. L. Lloyd, P. G. Kremsner, M. A. Missinou, M. English, K. Marsh, D. Kwiatkowski, A model for estimating total parasite load in falciparum malaria patients, Journal of Theoretical Biology 217 (2) (2002) 137–148.

[3] M. B. Gravenor, M. B. van Hensbroek, D. Kwiatkowski, Estimating sequestered parasite population dynamics in cerebral malaria, Proceedings of the National Academy of Sciences of the United States of America 95 (13) (1998) 7620–7624.

[4] L. B. Ochola, K. Marsh, Q. Gal, G. Pluschke, T. Smith, Estimating sequestered parasite load in severe malaria patients using both host and parasite markers, Parasitology 131 (4) (2005) 449–458.

[5] D. Bichara, N. Cozic, A. Iggidr, On the estimation of sequestred infected erythrocytes in plasmodium falciparum malaria patients, Mathematical Biosciences and engineering 11 (4) (2014) 741–759.

[6] K. H. Degue, D. Efimov, A. Iggidr, Interval estimation of sequestered infected erythrocytes in malaria patients, in: Proceedings of the 15th European Control Conference (ECC), Aalborg, Denmark, 2016.

[7] G. Goffaux, A. Vande Wouwer, O. Bernard, Continuous-discrete interval observers for monitoring microalgae cultures, Biotechnology Progress 25 (3) (2009) 667–675.

[8] K. H. Degue, D. Efimov, J.-P. Richard, Stabilization of linear impulsive systems under dwell-time constraints: Interval observer-based framework, European Journal of Control 42 (2018) 1–14.

[9] A. Rapaport, D. Dochain, Interval observers for biochemical processes with uncertain kinetics and inputs, Mathematical Biosciences 193 (2) (2005) 235–253.

[10] O. Bernard, J. L. Gouzé, Closed loop observers bundle for uncertain biotechnological models, Journal of Process Control 14 (7) (2004) 765–774.

[11] M. Kieffer, E. Walter, Guaranteed nonlinear state estimator for cooperative systems, Numerical Algorithms 37 (1-4) (2004) 187–198.

[12] F. Mazenc, O. Bernard, Asymptotically stable interval observers for planar systems with complex poles, IEEE Transactions on Automatic Control 55 (2) (2010) 523–527.

[13] S. Ifqir, D. Ichalal, N. Ait Oufroukh, S. Mammar, Robust interval observer for switched systems with unknown inputs: Application to vehicle dynamics estimation, European Journal of Control 44 (2018) 3–14.

[14] K. H. Degue, D. Efimov, J. Le Ny, E. Feron, Interval observers for secure estimation in cyber-physical systems, in: Proceedings of the 57th IEEE Conference on Decision and Control (CDC), Fontainebleau, Miami Beach, Florida, USA, 2018.

[15] M. Moisan, O. Bernard, J. L. Gouzé, Near optimal interval observers bundle for uncertain bio-reactors, Automatica 45 (1) (2009) 291–295.

[16] T. Raïssi, D. Efimov, A. Zolghadri, Interval state estimation for a class of nonlinear systems, IEEE Transactions on Automatic Control 57 (1) (2012) 260–265.

[17] D. Efimov, L. M. Fridman, T. Raïssi, A. Zolghadri, R. Seydou, Interval estimation for LPV systems applying high order sliding mode techniques, Automatica 48 (9) (2012) 2365–2371.

[18] F. Mazenc, O. Bernard, Interval observers for linear time-invariant systems with disturbances, Automatica 47 (1) (2011) 140–147.

[19] D. Rotondo, A. Cristofaro, T. A. Johansen, F. Nejjari, V. Puig, State estimation and decoupling of unknown inputs in uncertain LPV systems using interval observers, International Journal of Control 0 (0) (2017) 1–18.

[20] K. H. Degue, J. Le Ny, An interval observer for discrete-time SEIR epidemic models, in: Proceedings of the American Control Conference (ACC), Milwaukee, WI, USA, 2018.

[21] D. Efimov, A. Polyakov, J.-P. Richard, Interval observer design for estimation and control of time-delay descriptor systems, European Journal of Control 23 (5) (2015) 26–35.

[22] H. Ito, T. N. Dinh, Interval observers for global feedback control of nonlinear systems with robustness with respect to disturbances, European Journal of Control 39 (2018) 68–77.

[23] G. Hooker, S. P. Ellner, L. D. V. Roditi, D. J. D. Earn, Parameterizing state-space models for infectious disease dynamics by generalized profiling: measles in Ontario, Journal of the Royal Society Interface 8 (60) (2011) 961–974.

[24] E. I. Robinson, J. Marzat, T. Raïssi, Interval observer design for unknown input estimation of linear time-invariant discrete-time systems, IFAC-PapersOnLine 50 (1) (2017) 4021 – 4026, 20th IFAC World Congress.

[25] D. Efimov, L. Fridman, A hybrid robust non-homogeneous finite-time differentiator, IEEE Transactions on Automatic Control 56 (5) (2011) 1213–1219.

[26] L. Farina, S. Rinaldi, Positive Linear Systems: Theory and Applications, Wiley, New York, USA, 2000.

[27] H. L. Smith, Monotone Dynamical Systems: An Introduction to the Theory of Competitive and Cooperative Systems, Vol. 41 of Mathematical Surveys and Monographs, American Mathematical Society (AMS), Providence, 1995.

[28] C. Briat, M. Khammash, Interval peak-to-peak observers for continuous- and discrete-time systems with persistent inputs and delays, Automatica 74 (2016) (2016) 206–213.

[29] Y. Ebihara, D. Peaucelle, D. Arzelier, L1 gain analysis of linear positive systems and its application, in: Proceedings of the 50th IEEE Conference on Decision and Control (CDC), Orlando, Florida, USA, 2011, pp. 4029–4035.

[30] C. Briat, Robust stability analysis of uncertain linear positive systems via integral linear constraints: L_1- and L_∞-gain characterizations, in: Proceedings of the 50th IEEE Conference on Decision and Control (CDC), Orlando, Florida, USA, 2011, pp. 6337–6342.

[31] J. Löfberg, Automatic robust convex programming, Optimization methods and software 27 (1) (2012) 115–129.

[32] W. E. Collins, G. M. Jeffery, A retrospective examination of sporozoite- and trophozoite-induced infections with plasmodium falciparum in patients previously infected with heterologous species of plasmodium: effect on development of parasitologic and clinical immunity, American Journal of Tropical Medicine and Hygiene 61 (1) (1999) 36–43.

[33] M. Eichner, H. H. Diebner, L. Molineaux, G. M. Collins, W.E. Jeffery, K. Dietz, Genesis, sequestration and survival of plasmodium falciparum gametocytes: parameter estimates from fitting a model to malariatherapy data, Transactions of the Royal Society of Tropical Medicine and Hygiene 95 (5) (2001) 497–501.

[34] T. N. Dinh, H. Ito, Interval observers for continuous-time bilinear systems with discrete-time outputs, in: Proceedings of the 15th European Control Conference (ECC), Aalborg,Denmark, 2016.